21st Australasian Fluid Mechanics Conference
Adelaide, Australia
10-13 December 2018

Low cost high speed digital cameras for experimental fluid mechanics

D. J. Duke, T. Knast and D. Edgington-Mitchell

Laboratory for Turbulence Research in Aerospace & Combustion (LTRAC)
Department of Mechanical & Aerospace Engineering
Monash University, Clayton 3800, Australia

Abstract

Scientific high-speed digital cameras are essential for many experimental techniques in fluid mechanics. Their high cost is a major constraint on the capability and accessibility of flow diagnostic facilities. Advances in semiconductor manufacturing in recent decades have led to order of magnitude gains in the performance of the sensors used in these cameras. However, due to the small size of the market and the need for customisation and flexibility in design, the scientific camera market has not experienced the order-of-magnitude price decreases seen in the consumer sector. Recent supply side changes in the Chinese electronics market have led to an explosion of niche crowd-funded electronics. The impact of this shift in the electronics industry has not yet been fully appreciated, but it is now beginning to impact the scientific research community. In this paper, we present a technical overview and performance assessment of one of the first custom built crowd-funded scientific cameras, the *Chronos 1.4*. It is a low cost high-speed camera based on a *Luxima LUX1310* CMOS sensor package. It has 1280 $\times$ 1024 pixels at 6.6 μm pitch with a 1.2 μs global shutter, a bandwidth of 1.4 Gpix/s, flexible external triggering, and an open source development toolchain. It is capable of over 1000 frames/s (full sensor) and 38,565 frames/s with reduced field of view (336 $\times$ 96 pixels). We assess the performance of the *Chronos 1.4* with a well-characterised stroboscopic LED light source. Under the same conditions and with an identical optical setup, the *Chronos 1.4* compares favourably to two other scientific high-speed cameras. The small pixel pitch makes it ideal for highly magnified measurements. The low cost (USD $3k) and relatively small footprint is also ideal for multi-camera experiments and as an educational aid. We demonstrate its application in two experiments.

Themes: Experimental techniques & facilities

Introduction

In recent decades, high-speed digital cameras have become an essential component of nearly all fluid mechanics research facilities. High-speed imaging ($> 10^3$ frames/sec) with microsecond-range global shutter control is necessary for the imaging of fast fluid mechanical phenomena. Example applications include combustion experiments [1] and multiphase flows [2]. The ability of high-speed digital cameras to record orders of magnitude more consecutive images than mechanical devices such as drum cameras have made measurement techniques such as time-resolved particle image velocimetry (PIV) feasible [3].

The history of digital imaging has in general terms been a competition between two semiconductor design concepts; the charge coupled device (CCD) invented in 1969 and the complementary metal-oxide semiconductor (CMOS) active pixel sensor invented in 1985. The CCD uses a shift register to move charge off the array where it is then converted to a voltage which can be read by an analog to digital converter (ADC). Conversely, the CMOS sensor incorporates a charge amplifier into each pixel. A good comparison of these with relevance to fluid mechanics experimentation is given by Hain et al [4].

Until the mid 2000s, CCD sensors were preferred due to their superior noise and exposure control specifications. Recent improvements in dynamic range, global shutter capability [5] and lower cost have since seen CMOS sensors supplant CCDs in nearly all applications. The ability of the CMOS manufacturing process to include ADCs, readout electronics and programmable gain amplifiers (PGAs) on the imaging chip itself [6] gives a major advantage in speed and cost. The CMOS architecture allows the pixel charge to be rapidly reset between exposures [7].

The CMOS architecture has one major weakness. To minimise detector dead time for charge resetting, a penalty is paid in the form of image lag [8]. This is the phenomena of over-compensation of the pixel charge correction. It results in a shadow of the prior frame in subsequent frames. The effect is particularly pronounced if there are large changes in intensity between frames [9]. Cheap sensors can be particularly susceptible and any assessment of a low cost CMOS chip must therefore consider this effect.

Due to increased interest in high speed video in the entertainment and mobile phone industries, semiconductor fabricators are now mass producing high-speed CMOS chips that can compete with more custom-built scientific sensor packages. Simultaneously, the crowd-funding infrastructure established in North America over the last decade has led to a proliferation of low volume niche consumer electronics. This paper reviews the first high-speed digital camera using a mass-produced high-speed CMOS chip to be manufactured via crowd-funding. The *Chronos 1.4* (http://krontech.ca) is a Linux system on chip (SOC) build around the *Luxima LUX1310* CMOS package. It is battery powered and built into an aluminium handheld enclosure for portable use. It retails for about USD $3k depending on configuration. We assess its performance against two other scientific high speed cameras, and give two example applications.

Methodology

(a) (b)

Figure 1: Chronos 1.4 form factor and connectivity.

The *Chronos 1.4* form factor is shown in Fig. 1. Specifications are given in Table 1. These are compared to several other scientific high speed cameras. While the *Chronos 1.4* 's specifi-

Name	Sensor size Width	Height	Pixel pitch	Min. global shutter exposure	Max. frame rate at full-frame	Max. frame rate (absolute)	Internal memory	Sensor	Bandwidth (full frame)	Dynamic range (quoted)	Body dimensions Width	Height	Depth	Weight	Cost factor (approx.)
Chronos 1.4	1280 px	1024 px	6.6 µm	1.2 µs	1.057 kHz	38.565 kHz (640 × 96 px^2)	8-32 GB	12 bit CMOS	1.4 Gpix/s, 50 Gbit/s	56.7 dB	155 mm	96 mm	68 mm	1.06 kg	1×
IDT/Redlake MotionPro X3	2048 px	2048 px	12 µm	1 µs	1.000 kHz	64.000 kHz (1280 × 16 px^2)	4 GB	8 bit CMOS	1.3 Gpix/s 40 Gbit/s	59 dB	95 mm	95 mm	162 mm	1.9 kg	8 ×
Photron FastCam BC2HD	1280 px	1024 px	10 µm	2.76 µs	1.000 kHz	86.400 kHz (256 × 32 px^2)	32 GB	12 bit CMOS	4.2 Gpix/s 151 Gbit/s	57 dB	153 mm	165 mm	250 mm	7.3 kg	25 ×
PCO Dimax S4	2016 px	2016 px	11 µm	1.5 µs	1.279 kHz	152.811 kHz (240 × 16 px^2)	36 GB	12 bit CMOS	5.2 Gpix/s, 187 Gbit/s	64 dB	200 mm	160 mm	311 mm	7.9 kg	30 ×
Phantom v2511	1280 px	800 px	28 µm	0.3 µs	25.6 kHz	1 MHz (128 × 16 px^2)	96 GB	12 bit CMOS	26.2 Gpix/s 944 Gbit/s	not given	190 mm	280 mm	1775 mm	7.7 kg	50 ×
Photron FastCam SA-Z	1024 px	1024 px	20 µm	0.159 µs	20 kHz	21 MHz (128 × 8 px^2)	128 GB	12 bit CMOS	21 Gpix/s 755 Gbit/s	not given	262 mm	150 mm	376 mm	10.4 kg	50 ×

Table 1: Specifications of cameras compared in the tests (top three rows). For comparison, several other scientific high speed cameras from various manufacturers (not tested) are shown in italics.

cations are modest compared to many higher-end cameras, the cost to performance ratio is noteworthy. Its bandwidth-to-cost ratio is 3× higher than the next closest competitor. Along with the small form factor, this makes it attractive for multi-camera setups.

The *Chronos 1.4* 's system architecture is a Linux SOC connected to the *Luxima LUX1310* CMOS sensor via a field-programmable gate array (FPGA) which is initialised from memory at start-up. The FPGA controls the triggering, timing, and readout. These can be reconfigured from the SOC. The FPGA sends data from the dual 12-bit ADCs on the CMOS package to a standard laptop memory module, allowing easy upgrades and reducing cost. Data is saved to flash memory via USB or SD through the SOC. The camera is controlled via touch screen. Support for control and image download over gigabit ethernet are planned for a future firmware update.

The *Chronos 1.4* has a small pixel pitch (6.6 µm) and sensor footprint (8.4 × 6.8 mm) with a C mount and removable IR filter. This is advantageous for experiments such as digital holography and microscopic imaging, but less useful for large field of view experiments. There is no true double shutter mode. However, the external trigger does allow direct frame by frame triggering with both internal and external shutter gating down to 1.2 µs with 22 ± 6 ns jitter. There is a delay offset of 0.3 to 1.0 µs from the input TTL trigger to start-of-exposure; this varies with ROI and frame rate and is constant for a given set of operating conditions. The auxiliary clock output can be used to measure this delay. Further details are given in a forthcoming paper.

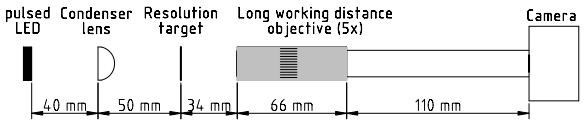

Figure 2: Optical configuration for the tests.

The first three cameras in Table 1 were compared using a single consistent optical setup (Figure 2). The light source was a pulsed green LED [10]. A 5× microscope was used to image a calibration target. The LED and camera exposure were controlled using a Beaglebone programmable real time delay generator [11]. The average flux was measured using a calibrated power meter (*Thorlabs PM100USB*), placed at the imaging sensor plane. The timing accuracy of the LED relative to the camera exposure time was confirmed using a reverse-biased PiN photodiode (*Thorlabs DET36A*). Tests were conducted for bright field signal to noise ratio with a constant train of 1 µs LED pulses at a frame rate of 1 kHz at various brightness levels. Dark-field and image lagging tests were conducted by strobing the light source, with 50 bright fields followed by 50 dark fields in a repeating pattern.

Results

Camera performance comparison

A sample image of a microscope resolution target with 2 µm spaced marker lines is shown in Figure 3. With a 5× infinity-corrected objective and 6.6 µm pixel pitch, resolution down to the diffraction limit of the imaging system is demonstrated without noticeable distortion.

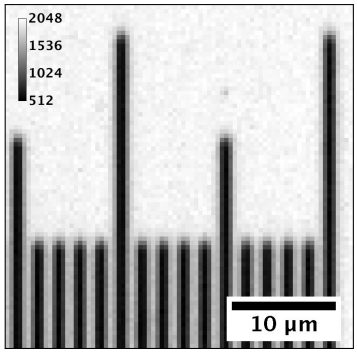

Figure 3: Sample cropped image from Chronos camera of microscope resolution target (12 bits, 4.85 px/µm).

The signal-to-noise ratio of the bright field intensity is shown in Figure 4. The *Chronos 1.4* is compared to the MotionPro X3, an 8-bit monochrome scientific camera, and the Photron BC2HD, a 12-bit colour camera. All tests were conducted with 1 µs exposures at 1 kHz. The error bars represent the combination of both spatial variation in SNR across the sensor, and uncertainty in the SNR for n=10^3 frames. Comparable performance is achieved for all cameras from 1 to 99% of saturation intensity. There is a loss of linearity for all cameras as they approach saturation; the effect is slightly more marked for the *Chronos 1.4* . The lower SNR of the BC2HD camera is mainly due to absorption in the Bayer filter, not the sensor response. The absolute sensitivity of the cameras was also tested. Once normalized by the pixel surface area, the *Chronos 1.4* was found to have a flux sensitivity equivalent to that of the Photron 12-bit camera of approximately 30 nJ/cm^2 (532 nm) at saturation.

Dark field dynamic range (i.e. dark noise) test results are given in Table 2. The advantages of high bit depth for the *Chronos 1.4* and BC2HD are mostly lost due to noise, although again it should be noted that the Bayer filter puts the BC2HD at a disadvantage and the reduced dynamic range is not an indication of any deficit in the sensor. The noise floor of the *Chronos 1.4* is primarily dictated by the fact that the sensor is air-cooled (the BC2HD is thermoelectrically cooled). A noticeable artefact in images from the *Chronos 1.4* is the presence of weak vertical banding in the noise field, as shown in Figure 5. This is likely due to the sensor readout design. The effect appears as a weak horizontal fluctuation in the noise floor. It exhibits

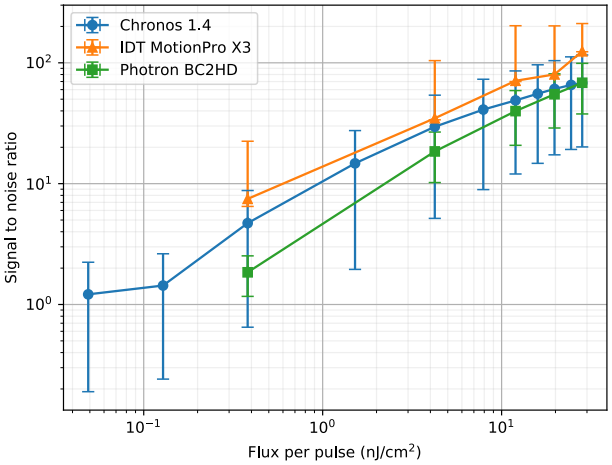

Figure 4: Signal to noise ratio of three high speed cameras using pulsed LED source in forward-scattering (1 µs at 1 kHz).

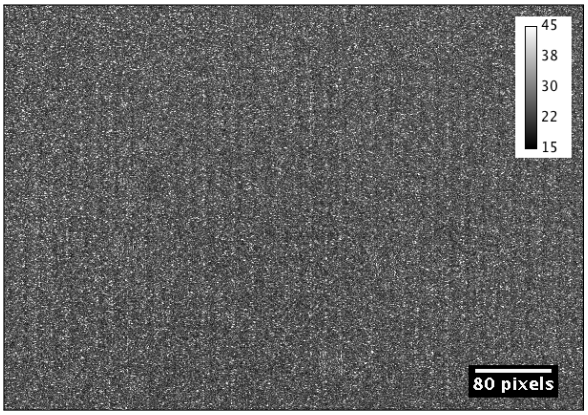

Figure 5: Spatial patterning of bright field standard deviation at the limit of saturation in forward-scattering for the *Chronos 1.4*

a periodicity of 16 pixels. This effect must be taken into consideration when small intensity changes are measured against a bright background.

The final series of tests compared the effects of image lag. This was achieved by imaging a sequence of 50 bright fields followed by 50 dark fields. The spatially averaged, ensemble averaged intensities for each frame after the last bright-field exposure (time, horizontal axis) are shown in Figure 6 for various incident intensity levels (vertical axis). Image lag causes the artificial dip in the average recorded intensity below the noise floor for the first frame after the last bright exposure. The effect becomes more pronounced as the incident intensity increases; this is inherent to all CMOS sensors. Results are not given for the MotionPro X3, as the bit depth masks the effect. Several key differences were observed between the BC2HD and the *Chronos 1.4* in lag performance. Like many high speed cameras, the BC2HD exhibits a shadow effect where the overcompensation occurs on a per-pixel basis. However the *Chronos 1.4* appears to exhibit a global effect where the entire sensor output drops below the noise floor after a bright exposure. This may be advantageous as the effect is easier to correct. The BC2HD also exhibits overshoot; i.e. an artifically higher intensity in the second frame after the last bright exposure. The *Chronos 1.4* does not exhibit this effect. Further details are given in a forthcoming paper.

Camera	Mean dynamic range	Standard deviation	Ideal dynamic range
Chronos 1.4	-59.2 dB	2.1 dB	-72 dB
Photron BC2HD	-43.5 dB	4.9 dB	-72 dB
MotionPro X3	-47.8 dB	4.9 dB	-48 dB

Table 2: Dark field dynamic range from tests of three cameras, as compared to the theoretical maximum dynamic range defined by the camera bit depth.

Example applications

Figure 7 shows a sequence images of a compressed air jet from a 2 mm diameter nozzle, conducted using a folded Z type schlieren imaging facility at LTRAC with parabolic mirrors. The exposure time was 5 µs and the frame rate was 1,057 frames/s. Figure 8 shows a sequence of images of a flash-evaporating R134a propellant spray with a nozzle exit diameter of 0.33 mm. A 72 mm macro-zoom lens was used. In this experiment the exposure time was 1 µs and the frame rate was 21,650 frames/s. At these frame rates, larger liquid structures can be individually tracked from frame to frame (red arrows). For both cases the light source was a pulsed LED of the same type as the calibration tests described above.

Conclusions

In this paper we have tested the performance of a low cost high speed CMOS camera with comparsion to an 8-bit monochrome scientific camera with comparable specifications, and a more modern colour high speed camera. The *Chronos 1.4* compares favorably in terms of linearity and signal to noise ratio, with slightly increased nonlinearity at high intensities. The camera's dark field dynamic range is also comparable. Both the *Chronos 1.4* and the BC2HD colour camera exibit a lagging effect when large intensity changes between frames occur; this is an unavoiable side effect of the CMOS architecture. However the Chronos does have an advantage in that the effect is global rather than pixel-local and this makes correcting it easier. The Chronos has one noticeable disadvantage in performance; a weak vertical patterning is seen in the RMS intensity for high incident intensity levels. This effect must be accounted for when measuring small changes in high intensity forward scattering experiments. The small pixel pitch makes the camera well suited to holographic and highly magnified experiments. The low cost of these cameras makes them an attractive option for multi-camera experiments and as a teaching tool.

Acknowledgements

The authors acknowledge the support of the Australian Research Council (DE170100018, LP160101845). Dr. Duke wishes to thank the technical support staff at Krontech and the users of the Krontalk forum (http://krontech.ca/forum) who provided useful technical advice. The authors wish to state that they derive no benefit from the promotion of any equipment or supplier mentioned in this paper, make no specific endorsements, and have no conflicts of interest to disclose.

References

[1] V Sick. High speed imaging in fundamental and applied combustion research. *Proc. Combustion Inst.*, 34(2):3509–3530, 2013.

[2] S T Thoroddsen, T G Etoh, and K Takehara. High-Speed Imaging of Drops and Bubbles. *Annu. Rev. Fluid Mech.*, 40:257–285, 2017.

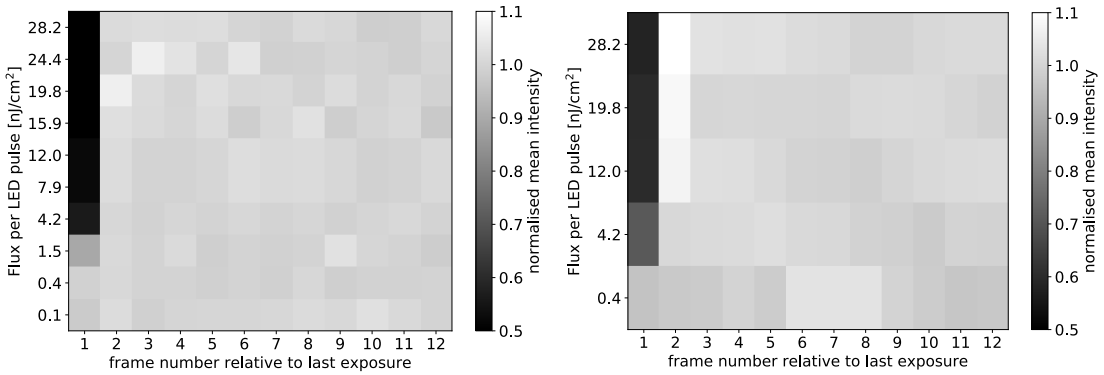

(a) Chronos 1.4

(b) Photron BC2HD

Figure 6: Image lag effect shown in terms of average intensity over the entire sensor, expressed as number frames after last bright-field exposure (horizontal axis) at various LED flux levels (vertical axis).

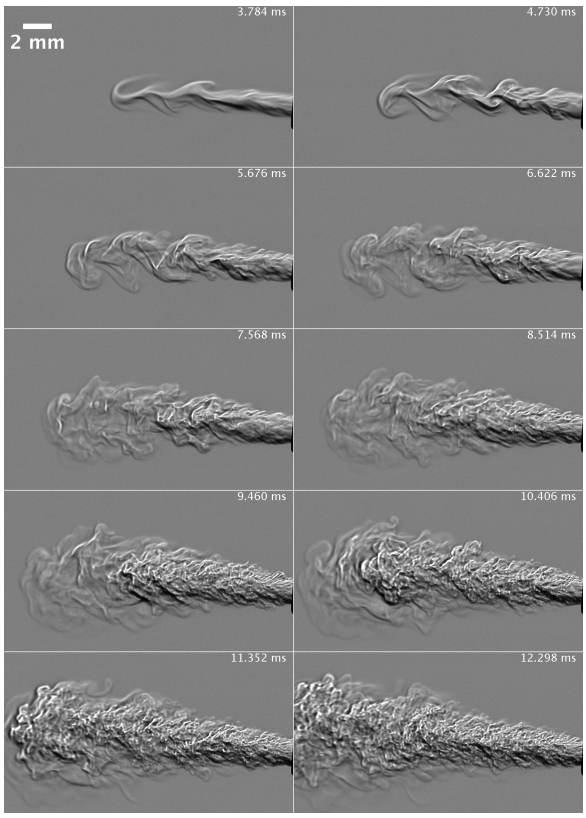

Figure 7: Cropped image sequence of a high-speed air jet in a Z-type schlieren setup using the *Chronos 1.4* at 1,057 frames/s.

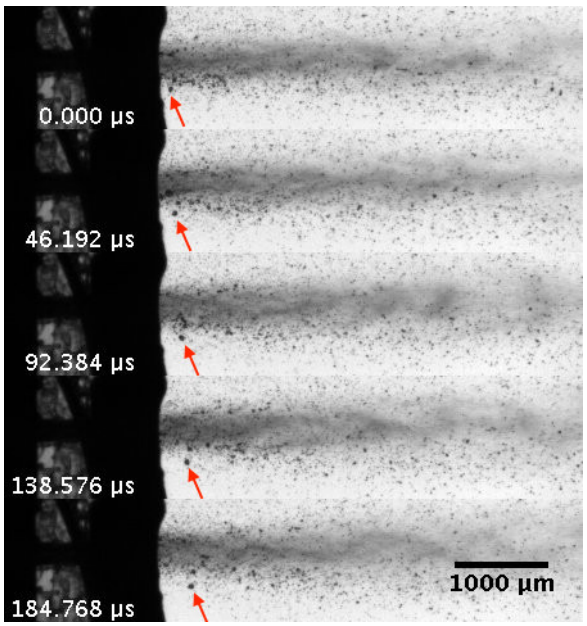

Figure 8: Cropped image sequence of a flash-evaporating medical spray using the *Chronos 1.4* at 21,650 frames/s.

1698, 1997.

[7] M El-Desouki, M J Deen, Q Fang, L Liu, F Tse, and D Armstrong. CMOS Image Sensors for High Speed Applications. *Sensors*, 9:430–444, 2009.

[8] E R Fossum. Charge Transfer Noise and Lag in CMOS Active Pixel Sensors. In *Proc. IEEE Workshop on Charge-Coupled Devices and Advanced Image Sensors*, Bavaria, Germany, 2003.

[9] J Manin, L M Pickett, and S A Skeen. Toward quantitative spray measurements using high-performance high-speed video cameras. In *Proc. ILASS-Americas 28th Annual Conference on Liquid Atomization and Spray Systems*, Dearborn, Michigan, USA, 2016.

[10] C E Willert, D M Mitchell, and J Soria. An assessment of high-power light-emitting diodes for high frame rate schlieren imaging. *Exp. Fluids*, 2012.

[11] M Fedrizzi and J Soria. Application of a single-board computer as a low-cost pulse generator. *Meas. Sci. Technol.*, 26:095302, 2015.

[3] E G Foeth, C W H van Doorne, T van Terwisga, and Wieneke B. Time resolved PIV and flow visualization of 3D sheet cavitation. *Exp. Fluids*, 40:503–513, 2006.

[4] R Hain, C J Kähler, and C Tropea. Comparison of CCD, CMOS and intensified cameras. *Exp. Fluids*, 42:403–411, 2007.

[5] M Furuta, Y Nishikawa, T Inoue, and S Kawahito. A High-Speed, High-Sensitivity Digital CMOS Image Sensor With a Global Shutter and 12-bit Column-Parallel Cyclic A/D Converters. *IEEE J. Solid State Circuits*, 42(4):766–774, 2007.

[6] E R Fossum. CMOS Image Sensors: Electronic Camera-On-A-Chip. *IEEE Trans. Electron. Dev.*, 44(10):1689–